PR8 Development on Neutron Imaging Application

Y. Saito

Research Reactor Institute, Kyoto University

1. Objectives and Allotted Research Subjects

Neutron imaging provides valuable information which cannot be obtained from an optical or X-ray imaging. The purpose of this project is to develop the imaging method itself and also the experimental environment for expanding the application area of the neutron imaging. The allotted research subjects are as follows:

ARS-1 Measurements of Multiphase Dynamics by Neutron Radiography (Y. Saito *et al.*)
ARS-2 Quantitative Measurement of Adsorbed Ethanol Amount in Activated Carbon Adsorber for Adsorption Heat Pump (N. Takenaka *et al.*)
ARS-3 Neutron Radiography on Tubular Flow Reactor for Supercritical Hydrothermal Synthesis of Nanoparticles (T. Tsukada *et al.*)
ARS-4 Characteristics of the Void Fraction under Transient Condition (H. Umekawa *et al.*)
ARS-5 Neutron imaging and optics development using simulation of VCAD Systems (Y. Yamagata *et al.*)
ARS-6 Water and Salt Distribution in a Rice Hull Medium under Sodium Chloride Solution Culture (U. Matsushima *et al.*)
ARS-7 Measurement of Water Content in Hardened Cement Paste by Neutron Imaging (T. Numao *et al.*)
ARS-8 Hydrazine Thickness Measurement by Neutron Radiography at a Catalyst Bed during Operation (H. Kagawa *et al.*)
ARS-9 Development of Neutron Imaging Devices (H. Iikura *et al.*)
ARS-10 Evaluation of the Moisture Movement in High-Performance Concrete Subjected to Heating (M. Kanematsu *et al.*)
ARS-11 Effect of gravity on coolant distribution in FGHP heat spreader (K. Mizuta *et al.*)
ARS-12 Study on Visualization of Organic Materials between Metals for Advance of Industrial Products (A. Uritani *et al.*)
ARS-12 Study on Visualization of Organic Materials between Metals for Advance of Industrial Products (A. Uritani *et al.*)
ARS-13 Visualization of Flow inside Fine Scale of Heat Pipe (Y. Tsuji *et al.*)

2. Main results and the contents of this report

In ARS-1, simultaneous measurements of water film distribution in an air-water two-phase flow were performed by using a Liquid Film Sensor (LFS) and a high frame rate neutron radiography to measure the film thickness distribution.

ARS-2 applied neutron radiography to heat transfer study on an adsorption refrigerator. In this ARS, visualization of adsorption amount distributions of ethanol in an activated carbon powder bed, using Umbra method in neutron radiography.

ARS-3 visualized the flow in a tubular flow reactor for supercritical hydrothermal synthesis of nanoparticle using neutron radiography. Measured mixing behaviors in the tubular flow reactor were compared with the size distributions of the synthesized nanoparticles.

ARS-4 was not performed this year.

ARS-5 was trying to develop a visualization technique for molding process by using neutron radiography and also a neutron focusing mirror. A 100mm rotational ellipsoid mirror was fabricated and its focusing performance was investigated at the CN-3 port

ARS-6 was not performed this year.
ARS-7 was not performed this year.
ARS-8 was not performed this year.
ARS-9 was not performed this year.

ARS-10 evaluated the water distribution in the hardened cement paste (HPC) using neutron radiography. In this study, experiments were carried out to investigate two-dimensional moisture movement in HPC.

ARS-11 applied neutron radiography to observe coolant distributions in a flat heat spreader (FGHP). The effect of gravity on coolant distribution in the FGHP was investigated by varying the heat load to the FGHP. At present experimental conditions, at least 0.1 mm thick liquid layer in the wick area exists in the middle plates of the FGHP.

ARS-12 applied neutron radiography to observe organic materials between metals for advance of industrial products. Experiments were conducted at the E-2 port and the test samples were bearing with and without grease. From the CT reconstruction of the neutron images, the grease distributions could be clearly observed.

ARS-13 applied neutron radiography to observe working fluid distributions in a house-made heat pipe, to understand the heat transfer process on a solid surface. Experiments were conducted at the E-2 port, and the heat pipe was visualized by changing he heat load from 6W to 30W. Cross sectional distributions of the working fluid could be measured by the neutron radiography.

採択課題番号 26P8　　中性子イメージングの高度化と応用　　プロジェクト
（京大・原子炉）齊藤泰司

PR8-1 Dynamic Observation of Two-Phase Flow using Neutron Radiography

Y. Saito and D. Ito

Research Reactor Institute, Kyoto University

INTRODUCTION: Neutron radiography (NRG) is a powerful tool for fluid flow visualization as well as two-phase flow research. Gas-liquid two-phase flows in a metallic pipe have been visualized clearly by using NRG. However, it would be still difficult to obtain dynamic information on such flows by NRG, because of insufficient neutron flux from neutron sources and poor efficiency of imaging devices. In this work, our imaging system was improved and a denoising method for acquired image sequence was developed for high frame rate NRG. Then, they were applied to air-water two-phase flow measurements in a narrow rectangular channel. In addition, a simultaneous measurement with an electrical conductance method was performed to investigate the detailed structure of the two-phase flow.

EXPERIMENTS: Experiments were performed at the B-4 supermirror neutron guide facility [1] of the Research Reactor Institute, Kyoto University. The neutron flux of the B-4 port is 5×10^7 n/cm^{2}s and the beam width and height at the beam exit are 10 mm and 75 mm, respectively. An imaging system for high frame rate NRG consists of a neutron converter, a dark box with a single mirror, a megapixel lens, an image intensifier and a high speed camera, as shown in Fig.1. NRG images acquired by this system were used to estimate the void fraction in the channel gap. Since the measured data include severe signal noises due to the statistical error in counting neutrons, a spatio-temporal filter was applied to enhance the quality of the void fraction distributions [2].
The test section has a rectangular cross section with 12 mm width and 2 mm gap. The vertical channel was placed at 1 m away from the neutron beam exit. The test fluids are air and tap water at room temperature. A liquid film sensor (LFS) [3] based on an electrical conductance measurement was applied to visualize the water film flowing in the narrow channel, which was installed on one side of the channel walls. LFS has 7×32 measurement points and the distance between the points was 1.5 mm. The temporal resolutions of both measurements were 200 Hz for NRG and 10,000 Hz for LFS.

RESULTS: The typical void fraction distributions measured by NRG are shown in Fig.2 (a) and (b). High void fraction values indicate where the bubble exists, and the size of bubbles could be roughly estimated from the distribution. However, several signal noises were found not only in the liquid phase region but also in the gas phase. Thus, the 3-D non-local mean filter was applied to the original images. The distributions filtered from Fig.2 (a) and (b) are shown in (c) and (d), respectively. The remarkable noises were reduced by the filtering process.

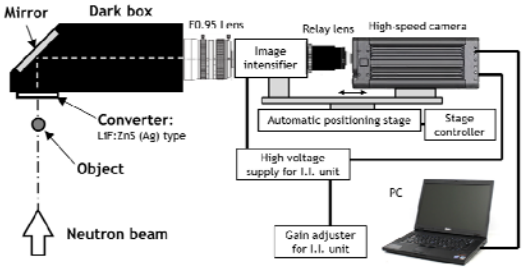

Fig. 1. High frame-rate neutron radiography system

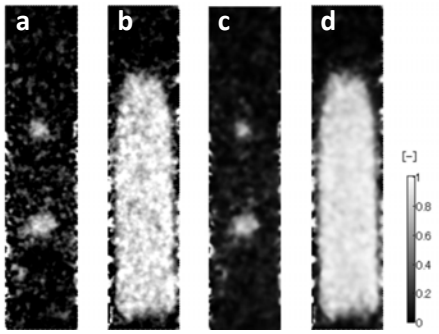

Fig. 2. Measured and filtered results of void fraction distribution

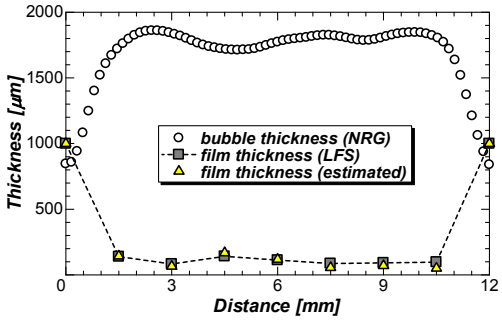

Fig. 3. Bubble and liquid film thickness profiles

The typical results obtained by a simultaneous measurement with NRG and LFS were shown in Fig.3. The horizontal profiles of the bubble and film thicknesses are represented. It is seen that the bubble occupies most of the gap in the channel. Thin film on the LFS could be measured by LFS. The film thickness on the opposing wall, which was estimated from the measured data of NRG and LFS, is also plotted in Fig. 3. This thickness profile agreed well with LFS result. Thus, the possibility of liquid film measurement on another wall was shown by the hybrid measurement with NRG and LFS.

REFERENCES:

[1] Y. Saito, *et al.*, Nucl. Instr. Meth. Phys. Res., A, **651** (2011) 36-41.
[2] Y. Saito and D. Ito, Proc. WCNR-10, (2014).
[3] D. Ito, *et al.*, Exp. Fluids., **51**-3 (2011) 821-833.

採択課題番号 26P8-1 中性子ﾗｼﾞｵｸﾞﾗﾌｨを用いた混相流のﾀﾞｲﾅﾐｯｸｽ計測に関する研究　プロジェクト（京大・原子炉）齊藤泰司、伊藤大介

PR8-2

Quantitative Measurement of Adsorbed Ethanol Amount in Activated Carbon Adsorber for Adsorption Heat Pump

H. Asano, K. Murata, N. Takenaka, H. Murakawa, K. Sugimoto, Y. Saito[1], D. Ito[1], Y. Kawabata[1]

Department of Mechanical Engineering, Kobe University
[1]Research Reactor Institute, Kyoto University

INTRODUCTION: Adsorption refrigerator is one of the efficient tools to recover waste heat at a low temperature. A design of the adsorber, in which refrigerant is adsorbed in adsorbent particle bed, is a key part for the improvement in the performance. To design the configuration of adsorber, it is required to clarify the adsorbed refrigerant distribution in the adsorbent particle bed during adsorption/desorption process. Neutron radiography was applied to visualize the adsorption amount distribution of ethanol in an activated carbon particle bed. The umbra method was applied to compensate the neutron scattering effect for quantitative measurement.

EXPERIMENTS: Activated carbon and ethanol was used as the adsorbent and refrigerant, respectively. The activated carbon MAXSORB® III produced by Kansai Coke and Chemical co., ltd. was used as the adsorbent. At first, the mass attenuation coefficient of liquid ethanol was measured using an ethanol step. Then, quantifiability in the measurement of adsorbed ethanol amount in activated carbon particle bed was evaluated by the measurement of an adsorbent step in dry and adsorption equilibrium condition. The adsorbent temperature was 21.5 °C and the pressure was 4.09 kPa. The umbra method using neutron absorber was applied to the quantitative measurement. A checked neutron absorber grid shown in Fig.1 was newly made for two-dimensional measurements. The offset value for an observed area can be measured by interpolating the brightness at the position covered by the neutron absorber surrounding the observed area. The width of the grid was 3 mm.

RESULTS: The measured results of the liquid methanol step are plotted with the symbol of ▲ in Fig. 2. The vertical axis shows the product of density, ρ, mass attenuation coefficient, μ_m, and thickness along the neutron beam, δ. The subscript r means ethanol as the refrigerant. A liner relationship between ethanol thicknesses and $\rho_r\mu_{m,r}\delta_r$ could be successfully obtained. The mass attenuation coefficient calculated from the gradient was 3.86 cm^2/g. For the measured results of adsorbed ethanol without the compensation plotted with the symbol of ○, the values seemed to become saturated due to the effect of neutron scattering and stray light in the camera system. It could be seen that the linear relationship could be obtained for the adsorbed ethanol by the umbra method as plotted with the symbol of ●. The measured values by neutron radiography was compared with those reported by El-sharkawy et al. [2] in Figure 7. They proposed the Dubinin–Astakhov equation for adsorbed ethanol amount on the same activated carbon based on the experimental results. It was confirmed that the adsorbed refrigerant amount could be measured quantitatively by the neutron radiography.

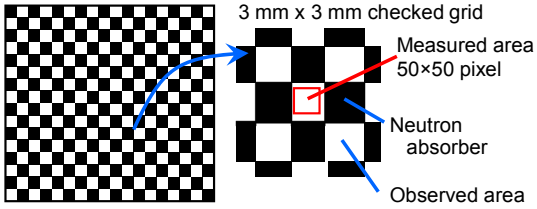

Fig. 1 Neutron absorber grid for umbra method.

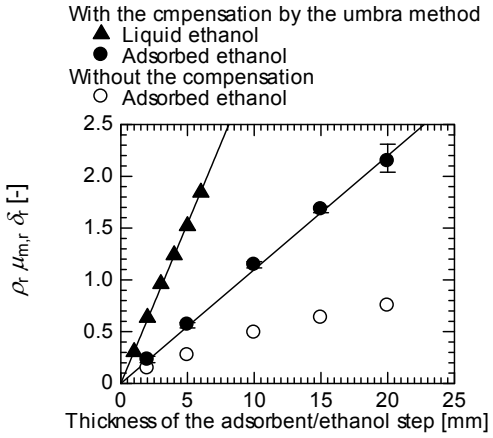

Fig. 2 Attenuation of neutron beam for various thickness of the adsorbent or ethanol step.

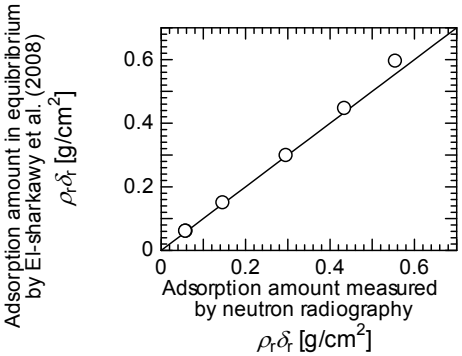

Fig. 3 Comparison of adsorption amount in equilibrium with the calculation by El-sharkawy et al.[2].

REFERENCES:

[1] N. Takenaka, et al., Nondestructive Testing and Evaluation, **16**-693 (2001), 345-354.
[2] I.I. El-Sharkawy, et al., Int. J. of Refrigeration, **31**-8 (2008), 1407-1413.

採択課題番号26 P8-2　　中性子ラジオグラフィによる機器内流動の可視化計測　　プロジェクト
（神戸大・工）竹中信幸、浅野等、村川英樹、杉本勝美（京大・原子炉）齊藤泰司、伊藤大介、川端祐司、（神戸大・工）村田健太、中村俊裕、北村信樹、米田久志、澤田将貴、古野正晃

PR8-3 Neutron Radiography on Tubular Flow Reactor for Supercritical Hydrothermal Synthesis of Nanoparticles

T. Tsukada, K. Sugioka, M. Kubo, K. Ozawa, S. Takami [1], T. Adschiri[2], K. Sugimoto[3], N. Takenaka[3], Y. Saito[4] and Y. Kawabata[4]

Dept. of Chemical Engineering, Tohoku University
[1]IMRAM, Tohoku University
[2]WPI-AIMR, Tohoku University
[3]Dept. of Mechanical Engineering, Kobe University
[4]RRI, Kyoto University

INTRODUCTION: Recently, a variety of metal-oxide nanoparticles have been synthesized by supercritical hydrothermal synthesis [1]. For the design and optimization of the process, it is important to acquire the correct knowledge about the mixing behavior of cold aqueous feed solution and supercritical water in a hydrothermal reactor. Therefore, we used neutron radiography to visualize the flow in a tubular flow reactor for supercritical hydrothermal synthesis, and investigated the effects of the flow rates of two fluids and reactor configurations on the mixing behavior in the reactor [2-4]. In this work, CeO_2 nanoparticles were actually synthesized by supercritical hydrothermal synthesis under the same conditions as those in neutron radiography, and then the size distributions of synthesized nanoparticles were discussed comparing with the flow and thermal fields observed by neutron radiography.

EXPERIMENTS: The tubular flow reactor, which was comprised of a Swagelok union tee and SUS316 tubes whose outer diameter and wall thickness were 1/8 inch and 0.71 mm, respectively, was used for synthesizing CeO_2 nanoparticles. Two streams of 10 mM $Ce(NO_3)_3$ aqueous solution and supercritical water were mixed and reacted at the T-junction in the reactor under approximately 25 MPa. The size distributions and average diameters of synthesized nanoparticles were evaluated using SEM (S-4800, Hitachi High-Technologies Co., Japan).

Neutron radiography of the tubular flow reactor was the same as that in our previous works [2-4], where a thermal neutron beam emitted from the B4 port in KUR was used. The imaging method of neutron radiography and subsequent analysis of the images were also similar to those in our previous work [3].

RESULTS: Figures 1 (a) and (b) shows SEM images and size distributions of nanoparticles synthesized using tubular flow reactors with two different configurations, when the flow rates of supercritical water and $Ce(NO_3)_3$ aqueous solutions were 8.0 and 1.0 g/min, respectively. In the figures, the temperature distributions obtained by neutron radiography are also shown. Octahedral CeO_2 nanoparticles are found to be synthesized hydrothermally in supercritical water. The size distribution of nanoparticles in (b) is much broader than those in (a), and the average sizes and the CV values of synthesized nanoparticles in (a) is smaller than those in (b). Here, the average size of an octahedral particle was defined by $(ls)^{1/2}$ with the lengths of major and minor axes, l and s, of particle. Such size distribution dependence of nanoparticles on reactor configuration is due to the difference in flow and thermal fields in the reactors. As the results of neutron radiography show, the stream of supercritical water flowing down through the vertical tube penetrates into the horizontal tube, and a thermally, density-stratified layer is generated in the horizontal tube of (a), while it seems from the temperature distributions in (b) that thermal buoyancy convection occupies the vertical tube just above the T-junction.

CONCLUSIONS: The relationship between the size distributions of synthesized nanoparticles and the mixing behaviors of the metal salt aqueous solution and supercritical water in the reactor was clarified by comparing between the results of supercritical hydrothermal synthesis and neutron radiography in the reactor.

REFERENCES:

[1] T. Adschiri *et al*., *Green Chemistry*, **13** (2011) 1380.
[2] S. Takami *et al*., *J. Supercrit. Fluids*, **63** (2012) 46.
[3] N. Takenaka *et al*., *Phys. Procedia*, **43** (2013) 264.
[4] K. Sugioka *et al*., *AIChE J*., **60**, (2014) 1168.

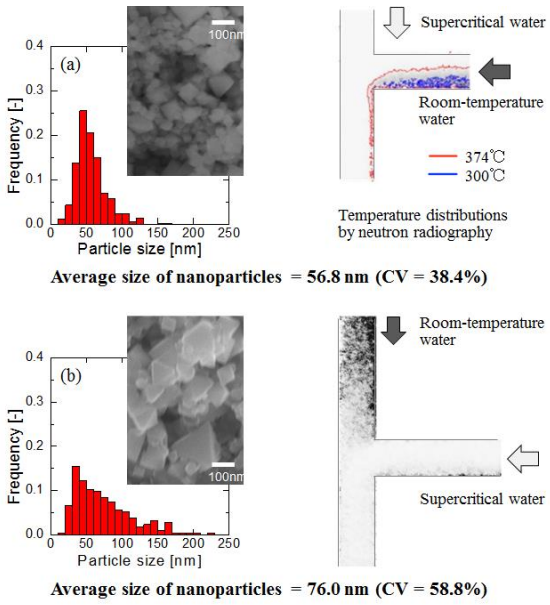

Figure 1 SEM images and size distributions of synthesized nanoparticles, and temperature distributions observed by neutron radiography.

採択課題番号 26P8-3 中性子ラジオグラフィを利用した超臨界水反応場の in-situ 観察 プロジェクト（東北大院・工）塚田隆夫、杉岡健一、久保正樹、小澤恭兵、（東北大・多元研）高見誠一、（東北大・WPI）阿尻雅文、（神戸大院・工）杉本勝美、竹中信幸、（京大・原子炉）齊藤泰司、川端祐司

PR8-4 Neutron imaging and optics development using simulation of VCAD Systems

Y.Yamagata[*1], S.Morita[*1],J.Guo[*1], J.Kato[*1], H.Yokota[*1], T.Sera[*1*2], Y.Kawabata[*3], Y. Saitoh[*3], M.Hino[*3], M.Sugiyama[*3], D.Ito[*3]

RIKEN Center for Advanced Photonics, RIKEN[*1], Osaka University[*2], Kyoto University Research Reactor Institute[*3]

INTRODUCTION:

VCAD System is a cluster of software codes, which can generate "real" object model in a computer and perform various numerical simulation. Those software codes include geometry conversion and input tools, 3D visualization, segmentation and mesh-generation tools, and various FEM-based simulation tools. The authors have been applied the neutron radiography data to VCAD systems to generate 3D geometry data and FEM analysis. Those software also include a simulation code for "real" optical components. We did a consideration about possible application of neutron radiography for the production process visualization for glass press mold lens and also conducted focusing experiments of small rotational ellipsoid mirror.

EXPERIMENTS:

(1)Consideration of visualization of molding process

It was not possible to carry out a neutron radiography, but we have considered the possibility of neutron radiography to visualization of glass molding process of aspherical lens. Many lenses for digital cameras today include at least a few aspherical lenses. Those aspherical lenses are manufactured by glass press molding using tungsten-carbide molding die at very high temperature of 500 to 900 degree. Since the process is done with high temperature inside tungsten carbide die, it was not possible to visualize the process. Total cross section of tungsten (W) is 23.1 for thermal neutron and considering that most glass material contain boron which has very high cross section, it may be possible to visualize the molding process through tungsten carbide die.

(2) Neutron beam focusing experiment

To manufacture a neutron focusing mirror with relatively lower cost and manufacturing time, the authors have started the development of neutron focusing mirror using metallic substrate.[1] The advantage of metallic substrate are easier mechanical handling and shorter manufacturing time. A 100mm rotational ellipsoid mirror was fabricated and focusing performance was tested at CN-3 port.[2]

RESULTS:

Fig. 1 shows the photo of the ellipsoid mirror through the manufacturing process. Fig.2 shows the beamline setup for ellipsoid mirror testing. The beam cam through pinhole (1mm) and U-shaped slit to eliminate the neutron beams that will not reflect on the mirror surface. The focused beam is detected by RPMT detector. It was possible to detect neutron beam focusing using this small mirror as shown in Fig.3. Focusing performance using VCAD software will be conducted in the near future.

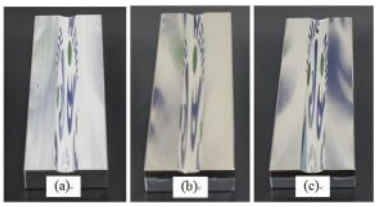

Fig.1 Manufactured ellipsoid mirror (a)aluminum substrate (b)NiP plated (c)polish finished

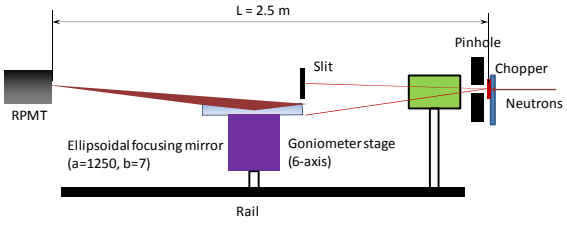

Fig.2 Experimental setup for neutron focusing experiment

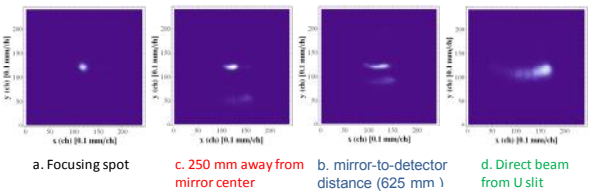

Fig.3 Focusing experiment result

REFERENCES:

[1] S.Takeda, H.Ohno, H.Sato, M.Furusaka, S.Morita, Y.Yamagata, M.Hino, "Development of an ellipsoidal neutron supermirror with metal substrate", International Workshop on Neutron Optics and Detectors, July (2013)

[2] J.Guo, S.Takeda, S.Morita, M.Hino, T.Oda, J.Kato, Y.Yamagata, and M.Furusaka, "New Fabrication Method for an ellipsoidal neutron focusing mirror with a metal substrate", Optics Express, Vol.22 No.20 DOI: 10.1364/OE.22.024666 (2014)

採択課題番号 26P8-5　　中性子ラジオグラフィによる工業製品の内部情報取得と　　プロジェクト
VCAD システムによるシミュレーション

（京大・原子炉）齊藤泰司、川端祐司、杉山正明、日野正裕、伊藤大介
（理研）山形豊、森田晋也、横田秀夫、世良俊博、加藤純一、池上祐司

PR8-5 **Evaluation of the Moisture Movement in High-Performance Concrete Subjected to Heating**

M. Kanematsu[1], S. Bae[1], T. Koyama[1], R. Inose[1],
N. Tuchiya[2], M. Tamura[3], Y. Nishio[3], T. Noguchi[3]
D. Ito[4] and Y. Saitou[4]

[1]*Department of Architecture, Tokyo University of Science*
[2]*Building Research Institute, Material Study Group*
[3]*Department of Architecture, The University of Tokyo*
[4] Research Reactor Institute Kyoto University

INTRODUCTION: High-performance concrete (HPC) has low water-to-binder ratio and it is vulnerable to the fire exposure, resulting in the explosive spalling of HPC surface at the early stage of fire. The spalling phenomena has been explained to occur due to the moisture pressure accumulated inside the pore of HPC [1]. However, the actual mechanism of the spalling has not been fully understood. To understand the detailed mechanism of spalling in HPC, 2-dimensional moisture movement in HPC subjected to heating was quantitatively assessed in this study.

EXPERIMENTS: The concrete specimen (100×100×20 mm^3) with water-to-binder ratio of 18 % was prepared. The initial moisture contents of the specimen was 14.1 % and the heating condition referred to the previous work [2].The TNRF in the B-4 beam-line of neutron flux $1\times10^7 n/cm^2$ was utilized for neutron radiography and the noise pixel in the images deviating more than 10 grayscale values were replaced by the median value of the pixels around the circle with 2-pixels radius.

RESULTS: Fig.1 presents 2-dimensional distribution of differential moisture contents of paste in the specimen per unit volume. The correlation between the change of water content and the intensity of transmitted neutron was examined using specimens with predetermined specific water contents. As shown in Fig.1, the moisture condensed areas were observed at the boundary of dried areas, moving up to the top with the temperature elevation. This phenomenon was also confirmed in our previous work, in the case of high strength mortar [2]. Furthermore, the presence of moisture condensed areas was observed around the coarse aggregates and the holes created for the internal temperature measurement, which is in good agreement with the previous numerical model [4]. The interfacial transition zone around the coarse aggregates is assumed to provide the space that the condensed moisture can pass through.The explosive spalling occurred for two times, at 1m26s and 1m27s, respectively. In the area of 0 to 5 mm from heating surface, moisture content increase was monitored with the value of 5.0×10^2 g/cm^3 6.0×10^2 g/cm^3 at each spalling. The influence of vapor pressure induced by moisture movement on the spalling phenomena of HPC will be further investigated in the future.

REFERENCES:

[1] T.Z.Harmathy, ASTM, Philadelphia, No.385, 75-95
[2] M.kanematsu et al, PJCI, vol36, No.1, 2014
[3] J. Zhao, Cem. Concr. Res., 65, 64-75, 2014

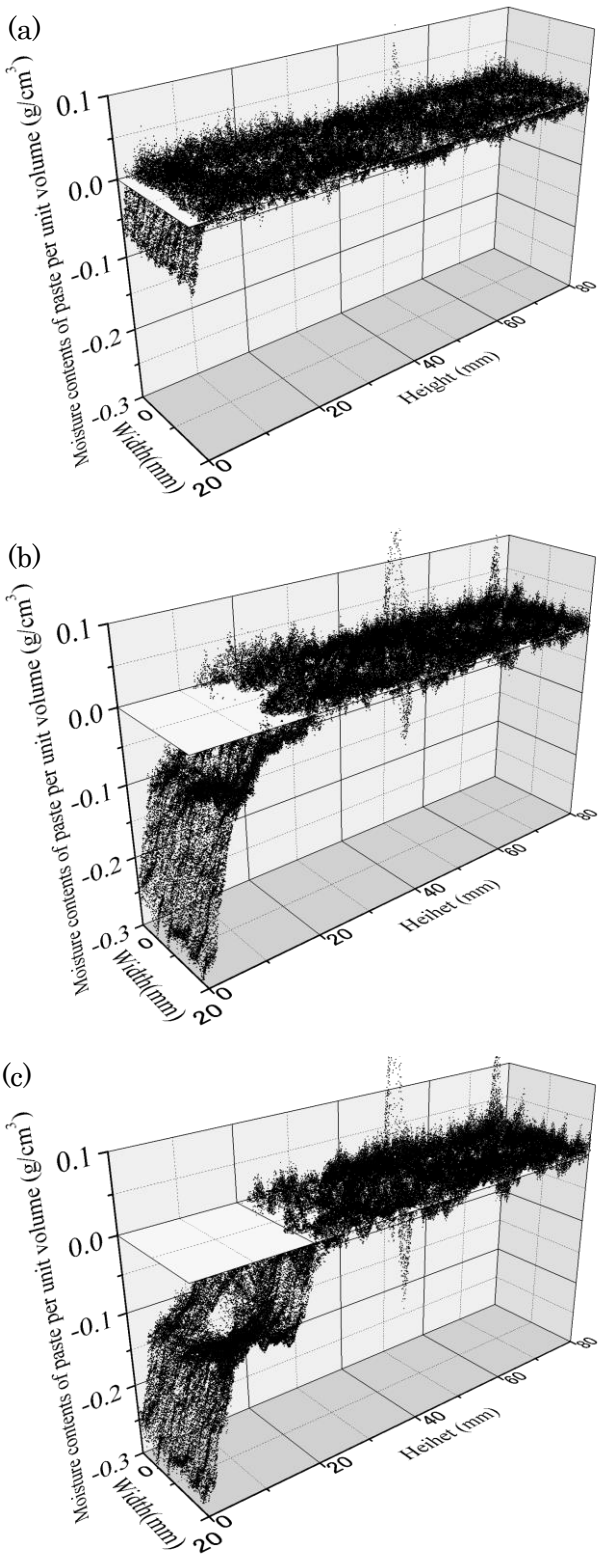

Fig.1 Two-dimensional distribution of differential moisture contents of paste of HPC per unit volume at (a) 1 min, (b) 4 min, and (c) 8 min after heating

採択課題番号26P8-10 高温加熱環境下における高強度コンクリートの水分移動の研究 プロジェクト
（東理大・理工）兼松学、Sungchul Bae、小山拓、猪瀬亮（建研・材料）土屋直子
（東大・工）田村政道、西尾悠平、野口貴文（京大炉）伊藤大介、齊藤泰司

PR8-6 Effect of Gravity on Coolant Distribution in FGHP Heat Spreader

K. Mizuta, Y. Saito [1], D. Ito [1]

Faculty of Engineering, Kagoshima University
[1] Research Reactor Institute, Kyoto University

INTRODUCTION: Recently, the importance of thermal management in electronic devices has become much higher than ever, because the lack in cooling ability in such devices leads to various reliability problems and low working efficiency. Particularly, in a light-emitting diode (LED) array, non-uniform temperature distributions caused by poor heat spreading ability of its substrate ruins the quality of lightning, because the light emitting efficiency of LED gets lowered with higher working temperature. To tackle with such problems in thermal management, vapor chambers would be one of the hopeful candidates as the substrate for its higher effective thermal conductivity compared with metal heat spreaders [1]. In an ordinary vapor chamber, however, it has been reported that the heat transfer characteristics are strongly affected by its installation posture, because the coolant circulation inside the vapor chamber is strongly affected by the gravity, which spoils the adoption of vapor chambers for the LED substrate. The authors have been trying to solve such problems by utilizing a newly developed vapor chamber called FGHP which is manufactured by precise etching technique by Molex Kiire Co., Ltd. located in Kagoshima, Japan. In this study, we investigated the gravitational effects on the coolant distribution in the FGHP by using neutron radiography at the Kyoto University Research Reactor (KUR).

EXPERIMENTS: Experiment was conducted at the E-2 port of the KUR, where the thermal neutron flux at the sample position was about 3×10^5 cm^2s at 5 MW operation. The size of the test sample of FGHP heat spreader was 65 mm square and 2 mm thick. The test sample was set vertically, which means that its bottom and top plate was placed parallel to the gravitational direction. A ceramic heater of $25\times25\times1.75$ mm^3 was attached to the central part of the bottom plate as a heat source, and the top plate was cooled by three pin-fin type aluminum heat sinks of 35×35 mm^2 under natural convection conditions. K-type thermocouples were utilized to measure both the surface temperature of the heat spreader and the atmospheric temperature to estimate the thermal resistance of the FGHP. A CCD camera (BU-53LN, BITRAN Co. Ltd.) was utilized, which has 4008×2672 pixels and ^{6}LiFZnS (50 μm thickness) was used as a scintillator screen. The spatial resolution was 9.0 μm/pixel at the present system setup, however, the effective spatial resolution was about 50 μm/pixel due to the scintillator screen characteristics.

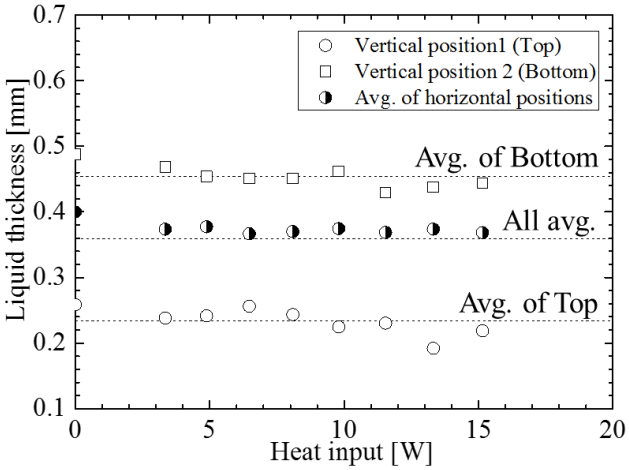

Fig. 1. Variation of the liquid thickness in the wick area with input power.

Neutron imaging of the sample was performed at the 1 MW operation mode of the KUR and the exposure time was 300 s. Neutron images of the sample were utilized to calculate liquid thickness in the FGHP. The effect of gravity on the coolant distribution was evaluated by the calculated liquid thickness in the wick area at different positions as follows:

1. Vertical position 1 (Top),
2. Vertical position 2 (Bottom),
3. Horizontal position 1 (Left),
4. Horizontal position 2 (Right).

Interrogation window size was 0.4×1.5 mm^2 at each position.

RESULTS: Figure 1 shows the variation of liquid thickness with heat input. As shown in Fig. 1, the measured values of the liquid thickness in the wick area take the smallest at the top and the largest at the bottom positions. The measured values range from 200 to 480 μm and increases along with the gravitational direction. However the liquid thickness remains nearly constant regardless of the heat input. From the design of the inner structure of the FGHP heat spreader, the maximum liquid thickness in the wick area can be estimated as 0.6 mm (about 0.1 mm in the middle plates and 0.5 mm in the top and the bottom plates), therefore, at least 0.1 mm thick liquid layer would be considered to cover the surface of the middle plates as the wick structure, which may suggest the surface of the whole wick area does not dry out even when the FGHP is installed in the vertical posture.

REFERENCES:

[1] J. C. Wang, Int. J Heat and Mass Trans., **53** (2010) 3990-4001.

採択課題番号 26P8-11　　フラットヒートパイプ型ヒートスプレッダ内部における冷媒挙動に関する研究　　プロジェクト

（鹿児島大・工）水田 敬（京大・原子炉）齊藤 泰司、伊藤 大介

PR8-7

Study on Visualization of Organic Materials between Metals for Advance of Industrial Products

K. Hirota[1], A. Uritani, K. Watanabe, A. Yamazaki, D. Sugimoto, Y. Kiyanagi, Y. Shiota, H. M. Shimizu[1], G. Ichikawa[1], M. Kitaguchi[2], Y. Saito[3]

Graduate School of Engineering, Nagoya University
[1] Graduate School of Science, Nagoya University
[2] Kobayashi-Maskawa Institute, Nagoya University
[3]Research Reactor Institute, Kyoto University

INTRODUCTION: The machinery industry products including automobile and aircraft are progressing to high performance and high precision. One of the desired technique in these development fields of state-of-art technology products is visualization of organic film (oil film grease, etc.) exist between metals. In the present work we explore the possibility of observation of the characteristics(shape, nature and the distribution of thickness) of the organic skin and its dynamic changes.

EXPERIMENTS: The measurement was done at E2 beam port in the reactor room. Bearings and an oil pump are using for the sample materials. The CCD system is Bitran BU-53LN and the scintillator is ^{6}Li/Zns(Ag) of thickness 200 μm, which is prepared RIKEN group and normally equipped at E2. The neutron (static) radiography image and CT reconstruction images were taken for both bearings and oil pomp. The CT reconstruction system is also equipped at E2. The typical exposure time is one minute for static image in 1 MW mode. This exposure time is decrease to 1/5 at 5MW mode. In the case of CT measurement, 30 seconds exposure time and 300 images, which are corresponding to 0.6-degree sample rotation step, are taken.

RESULTS: Figure 1 shows the neutron radiography image of bearings. These bearings are all commercial products. Half of these bearings are removed grease. White color area means that the neutron beam is easily transmitted, and black area means absorption. Neutron beam is expected to be well aborted by grease because of including of hydrogen. Clear grease image were available to find by comparing the picture between with and without grease. Figure 2 shows the CT reconstruction image of bearing include grease. Black-and-white shade is inverted to fig. 1. White area indicated the grease in the case of fig. 2. The grease skin is available to see between the boll and the frame of the bearing.

We want to observe how to move the grease with bearing rotation as next plan.

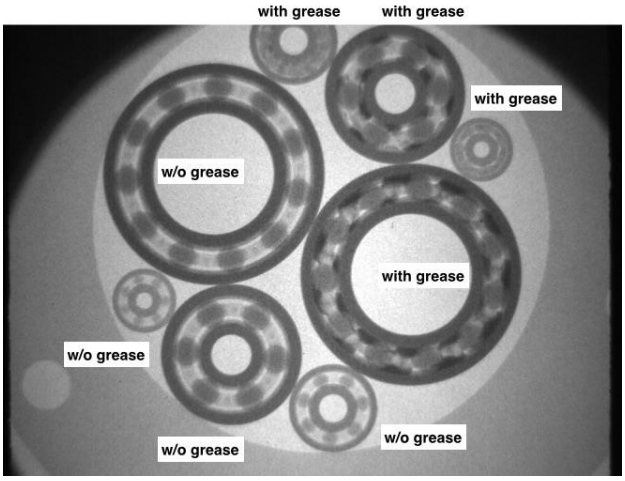

Fig. 1. Neutron radiography image of the bearings. Half of these bearings are removed the grease.

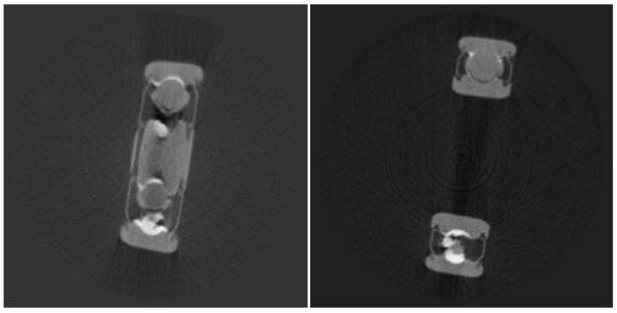

Fig. 2. CT reconstruction image. Black-and-white shade is inverted to fig. 1.

採択課題番号 26P8-12　　工業製品の高度化に資するための金属間有機物の可視化に関する研究　　プロジェクト

（名古屋大・工）瓜谷章、渡辺賢一、山崎淳、杉本大、鬼柳善明、塩田佳徳、（名古屋大・理）清水裕彦、広田克也、市川豪、（名古屋大・KMI）北口雅暁、（京大・原子炉）齊藤泰司

PR8-8 Visualization of Flow Inside Fine Scale Wick of Heat Pipe

Y. Tsuji, T. Ito, M. Ogasawara, S. Yanagisawa,
M. Tamaki[1], D. Ito[2] and Y. Saito[2]

Graduate School of Engineering, Nagoya University
[1]Department of Energy Engineering and Science
Graduate School of Science, Kyoto University
[2]Research Reactor Institute, Kyoto University

INTRODUCTION: We study the heat transfer process on the solid surface covered with liquid water. It is not clearly understand how the heat transfer is enhanced by changing the condition of solid surface, characteristics of liquid and flow conditions. We study the heat pipe (Fig.1) as the simple equipment to study the heat transfer process, and the following points are focused. (1) Character of solid surface is changed, such as a water-repellent coat, a hydrophilic coat, and/or a monomolecular film are added over the solid surface. (2) To change the solid surface condition as a complicated shape (wick). Such as porous media is attached on the surface and visualize the boiling process inside it. The boiling process is significantly affected by a porous shape and surface condition. (3)Heat transfer is measured independently, and it is compared with boiling process inside the porous media is visualized by NRG.

The purpose of this study is to enhance the heat transfer and understand its physical process by analyzing the visualized images by NRG.

EXPERIMENTS: House-made heat pipe is operated with supplying the heat by the Peltier module. We change the conditions of heat transfer with monitoring the NRG image. The heat pipe is made of aluminum, whose dimension is 20×110×110mm. Heater power is varied from 6 W to 30W, and the temperature of heater section changes from 40℃ to 70℃. The maximum inside pressure is 36 kPa.

In this measurement, we have to check the basic performance of NRG technique for observing the air, vapor and water states and their motions. Working fluid is water (20ml), and three different amounts of air (0, 5, 10ml) are supplied inside the heat pipe. The E2 beam port was used for NRG experiments.

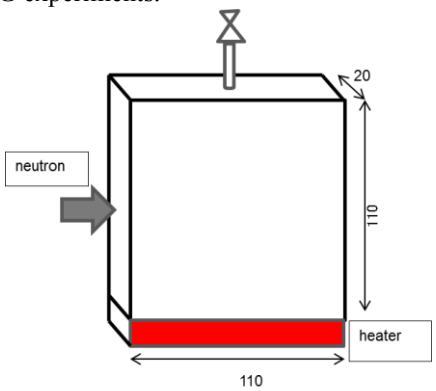

Fig.1 Schematic view of experimental setup

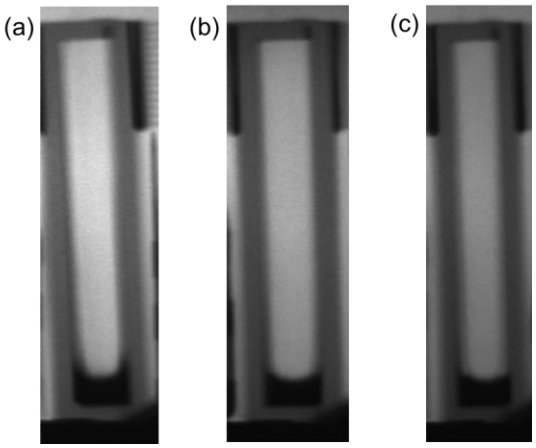

Fig.2 Neutron radiography image. (a) air=0ml, (b)air=5ml, (c)air=10ml.

RESULTS: The neutron radio grapy images are shown in Fig.2. We hope to observe the air, vapor and water phases inside the heat pipe, however it was difficult to distinguish them clearly. The water phase (black) is suppressed in (c) compared with (a) condition. This may be due to the increase of vapor pressure by adding the air. As the heat pipe is slightly tilted along the side wall, we can observe the thin liquid film flowing from top to down. This is caused by the liquid (water) condensed at the upper region and return to the bottom. On the left-side wall, the liquid film is thicker than that of right wall.

For the qualitative analysis from the digitized image intensity, the effect of aluminum wall is removed. We visualized the heat pipe, which does not contain the working fluid. By using this calibration image, background image is subtracted, that is usually adopted as NRG procedure. Figure 3 shows the averaged intensity profiles along the vertical direction of heat pipe. The intensity corresponds to the ratio of water averaged over the cross direction. The different colors show the conditions (a), (b), and (c), respectively. At the bottom region close to heater, the intensity of (a) shows the smaller value than other conditions. This indicates the water region remains much more in (a) condition. However, we can not distinguish the vapor and air regions. For the final purpose of our research, the vapor region should be distinguished from other states (water and air phases). The present techniques are revised in the next stage.

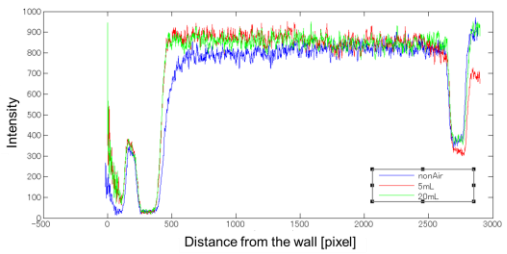

Fig.3 NRG intensity profiles along the heat pipe.

採択課題番号 26P8-13　微細ウイック内流動のＮＲＧによる可視化に関する研究　プロジェクト（名大院工）辻義之、伊藤高啓、小笠原克、玉置昌義（京大・原子炉）齊藤泰司